Diabetes, Metabolic Syndrome and Obesity

Dovepress

open access to scientific and medical research

Open Access Full Text Article

ORIGINAL RESEARCH

RETRACTED ARTICLE: Network Pharmacology, Molecular Docking, and Experimental Verification to Reveal the Mitophagy-Associated Mechanism of Tangshen Formula in the Treatment of Diabetic Nephropathy

Yinfeng Chen*, Xiaying Wang*, Jie Min, Jie Zheng, Xuanli Tang, Xiaoling Zhu, Dongrong Yu, De Jin

Department of Nephrology, Hangzhou TCM Hospital Affiliated to Zhejiang Chinese Medical University, Hangzhou, Zhejiang Province, 310007, People's Republic of China

*These authors contributed equally to this work

Correspondence: Dongrong Yu; De Jin, Department of Nephrology, Hangzhou TCM Hospital Affiliated to Zhejiang Chinese Medical University, Hangzhou, Zhejiang Province, 310007, People's Republic of China, Email yudr68@163.com; 826[illegible]1274@qq.com

Purpose: This study investigated the mechanism of TSF in treating DN through network pharmacology, molecular docking, and experimental validation.

Methods: To identify critical active ingredients, targets, and DN genes in TSF, multiple databases were utilized for screening purposes. The drug-compound-target network was constructed using Cytoscape 3.9.1 software for network topological analysis. The protein interaction relationship was analyzed using the String database platform. Metascape database conducted enrichment analysis on the key targets using Gene Ontology and the Kyoto Encyclopedia of Genes and Genomes. The renoprotective effect was evaluated using a mouse model of diabetic nephropathy (db/db mice) that occurred spontaneously. Validation of the associated targets and pathways was performed using Western Blot (WB), Polymerase Chain Reaction (PCR), and Immunohistochemical methods (IHC).

Results: The network analysis showed that the TSF pathway network targeted 24 important targets and 149 significant pathways. TSF might have an impact by focusing on essential objectives such as TP53, PTEN, AKT1, BCL2, BCL2L1, PINK-1, PARKIN, LC3B, and NFE2L2, along with various growth-inducing routes. Our findings demonstrated that TSF effectively repaired the structure of mitochondria in db/db mice. TSF greatly enhanced the mRNA levels of PINK-1. WB and IHC findings indicated that TSF had a notable impact on activating the PINK-1/PARKIN signaling pathway in db/db mice, significantly increasing LC3 and NRF2 expression.

Conclusion: Our results indicate that TSF effectively addresses DN by activating the PINK-1/PARKIN signaling pathway and enhancing Mitochondrial structure in experimental diabetic nephropathy.

Keywords: tangshen formula, diabetes nephropathy, network pharmacology, mitophagy, PINK1/Parkin pathway

Introduction

Diabetic Nephropathy (DN) is widely recognized as a significant contributor to end-stage renal diseases globally.[1] The prevalence of DN in China also shows a rapid growth trend. From 2009 to 2012, the prevalence of diabetic nephropathy in patients with type 2 diabetes in China was 30–50% in community patients.[2,3] Early identification, regulation of blood sugar levels, and strict control of blood pressure are the currently recommended approaches for managing DN, with a preference for utilizing angiotensin-converting enzyme inhibitors/angiotensin receptor blockers.[4] However, it is well known that the progression of DN involves multiple mechanisms, such as the elevated activity of polyol and hexosamine pathways, excessive advanced glycation end products (AGEs), and protein kinase C (PKC) isoforms, and inadequate

Received: 29 October 2023
Accepted: 1 February 2024
Published: 13 February 2024

antioxidant defense.[5,6] These pharmacological treatments for DN may not effectively delay diabetic kidney damage in many clinical practices.

In the past few years, a growing amount of research has examined the significance of mitophagy in DN.[7,8] Mitophagy, a specific type of autophagy responsible for eliminating damaged or surplus mitochondria, is crucial for maintaining the balance of cellular energy and is involved in kidney function.[8,9] According to recent studies, it has been indicated that as kidney damage advances, mitophagy may become overwhelmed or hindered, resulting in the accumulation of mitochondrial fragments and ultimately causing the death of cells.[8] This is confirmed in previous studies. In the model of type 1 diabetes in Ins2±AkitaJ mice, the renal function and tubular interstitial fibrosis could be enhanced by administering MitoQ orally. This enhancement is strongly associated with the upregulation of PINK/Parkin pathways, which are crucial in regulating mitophagy in renal tubules.[7,8] In the db/db mouse, activating PINK1/Parkin signaling by Astragalus could safeguard the kidneys against inflammation injuries.[9–12] These prove the pivotal roles of the PINK1/Parkin pathway as a cellular mitophagy gatekeeper in DN. Furthermore, the progression of DN can be delayed or improved by a therapy that controls mitophagy and the PINK1/Parkin pathway.

Traditional Chinese medicine (TCM) has extensively treated DN and has shown positive clinical results.[13,14] The Tangshen formula (TSF) is a classic Chinese herbal formula created by experts from the Department of Nephrology at Hangzhou Hospital of Traditional Chinese Medicine. TSF has been used in clinical practice for over forty years to treat DN, yielding positive outcomes. It consists of Huangqi (HQ, *Radix Astragali seu Hedysari*), Danggui (DG, *Radix Angelicae Sinensis*), Jixuecao (JXC, *Centella asiatica (L.) Urb.*), Fangji (FJ, *Radix Stephaniae Tetrandrae*), Taoren (TR, *Semen Persicae*), and Dahuang (DG, *Radix et Rhizoma Rhei*). All the plants in the TSF were formally identified and confirmed based on clinical practice by experts at Hangzhou Hospital of Traditional Chinese Medicine. All the names of plants in TSF were formally identified and confirmed at http://www.theplantlist.org. No additional approval was required for all herbal studies in this work. A prior investigation indicated that TSF decreases proteinuria and enhances renal function in individuals diagnosed with DN.[15] Nevertheless, the complete understanding of the TSF mechanism for DN remains uncertain.

Network pharmacology is an approach and technique used to identify essential substances and targets and uncover associations between drugs, genes, and diseases.[16] Regulating the mitophagy mediated by PINK-1/PARKIN has been demonstrated in a previous study to be effective in preventing DN.[17,18] Using network pharmacology, molecular docking, and animal experimental validation, this study is the pioneer in revealing the beneficial elements, possible targets, and mechanisms of TSF in treating DN through mitophagy. Figure 1 displays the depicted flow chart for this study.

Materials and Methods

Screening of Active Components and Targets of TSF

The Traditional Chinese Medicine Systems Pharmacology Database and Analysis Platform (TCMSP) (https://old.tcmsp-e.com/tcmsp.php) was utilized to explore the components of TSF, employing the keywords "Huangqi (Radix Astragali seu Hedysari)", "Danggui (Radix Angelicae Sinensis)", "Jixuecao (Centella asiatica (L.) Urb.)", "Fangji (Radix Stephaniae Tetrandrae)", "Taoren (Semen Persicae)", and "Da Huang (Radix et Rhizoma Rhei)". The set parameters are as follows: oral bioavailability (OB) must be equal to or greater than 30%, and drug-likeness (DL) must be equal to or greater than 0.18. To forecast the potential targets of the candidate ingredients, TCMSP and Swiss Target Prediction (http://swisstargetprediction.ch/) were employed. The UniProt database standardized the target nomenclature (https://www.uniprot.org/).

Screening of DN and Mitophagy-Related Targets

The potential genes that DN and mitophagy may affect were acquired from the Online Mendelian Inheritance in Man (OMIM) database (https://omim.org/); DisGeNET database (https://www.disgenet.org/); Pharmacogenetics and Pharmacogenomics Knowledge Base database (PharmGkb), (https://www.pharmgkb.org/), DrugBank (https://go.drugbank.com/) and the Therapeutic Target & Drug Data (TTD) database (https://db.idrblab.net/ttd/).

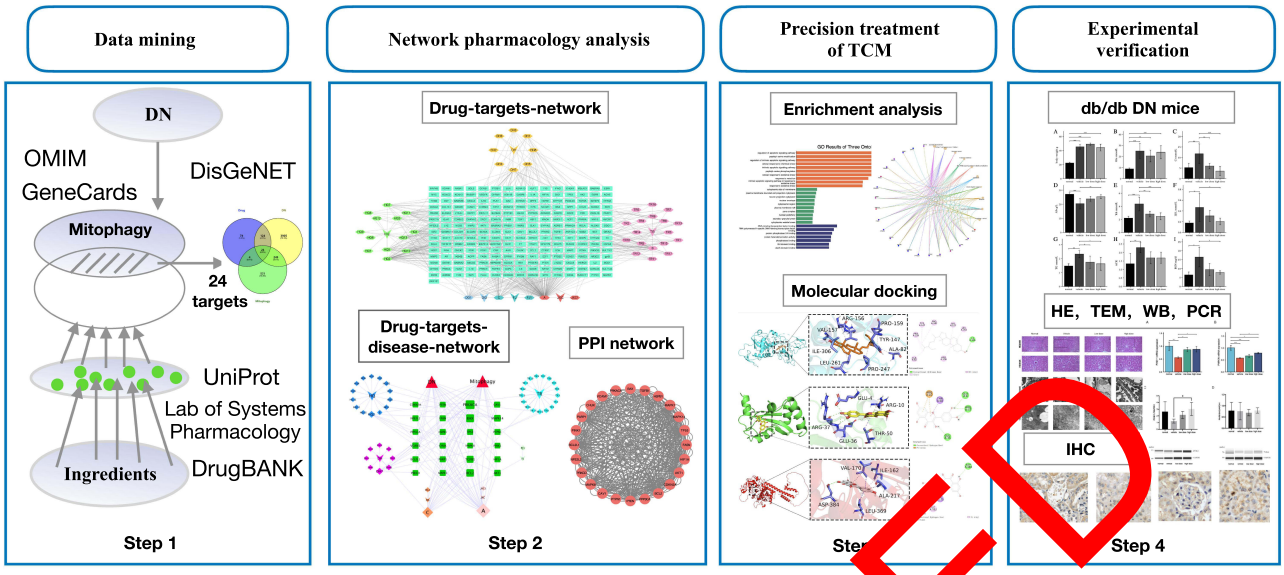

Figure 1 The study flowchart. Schematic diagram of the integrated pharmacology strategy approach that combines qualitative analysis of components, network analysis, molecular docking and vivo experimental verification to investigate the mechanisms of TSF treatment for DN.

Construction of the TSF-Component-Target-DN Network Alongside the Protein-Protein Interaction (PPI) Network

By creating a Venn diagram, we acquired the common targets of the TSF when treating DN. Cytoscape 3.8.1 software was used to import data regarding the active component of the TSF and the shared genes of the TSF and DN. To build a PPI network, the overlapping goals of TSF and DN were imported into the STRING database (https://cn.string-db.org/). A threshold of 0.90 was set for the minimum interaction score. Then Cytoscape 3.8.1 software was utilized to acquire the PPI network graphs of TSF for DN.

GO and KEGG Enrichment Analysis of TSF Components and DN Targets

The identified shared target genes were entered into the Metascape Database (http://metascape.org/) for Annotation, which includes the Kyoto Encyclopedia of Genes and Genomes (KEGG) and Gene Ontology (GO). We set the parameter as "H species". The most highly ranked outcomes from GO and KEGG enrichment analyses were filtered based on their physiology and pharmaceutical relevance significance. The above results were visualized using R 4.01 software.

Molecular Docking Validation

Sybyl software was used to dock critical targets and key ingredients previously identified by network pharmacology. The software Sybyl-X 2.1.1 was employed to create small molecule compounds in mol2 format. The compute module was utilized to optimize the generated small molecule compounds, specifying a maximum of 10,000 iterations. The crystal structures of important targets screened in the previous step were obtained in PDB format using the RCSB PDB database (https://www.rcsb.org/). Next, the surflex-dock geom docking mode in Sybyl-X 2.1.1 was employed to prepare ligands and proteins for molecular docking. Furthermore, the outcomes of the molecular docking were visualized using Pymol 4.6.0 software.

Experimental Validation

After a week of acclimatization, the average body weight of the db/m mice was 22.30 ± 1.20 g, while the db/db mice had an average body weight of 43.95 ± 3.24 g. We divided 24 db/db mice into three groups randomly: the model group (db/db, n = 8), the low-dose treatment group (db/db + L-TSF at 6.79 g/kg/d, n =8), and the high-dose treatment group (db/db + H-TSF at 20.36 g/kg/d, n =8). Eight mice (n =8) were used as the control group in the experiment. We provided

a high-fat diet to db/db mice for eight weeks. Throughout the investigation, every mouse was provided unrestricted water and food availability. We measured the animals' physical and chemical parameters, which included weight, urine samples collected in a metabolic cage (UACR, urine albumin-creatinine ratio), and blood samples (glucose, creatinine, urea, blood lipid, and albumin levels). Approval for this study was obtained from the Ethics Committee of Zhejiang Chinese Medicine University (IACUC-20210315-05). The principles of laboratory animal welfare follow the 3R principle: Reduction, Replacement, and Refinement. We minimize the number of tests and animals used while ensuring the quantity and accuracy of data information. GemPharmatech Co., Ltd (Nanjing, China) provided eight-week-old male mutant diabetic (db/db) mice (LEPR gene knockout) and non-diabetic (db/m) littermates (control) (LEPR wild-type).

Abdominal dissection promptly separated and extracted the kidneys, which were then weighed and prepared for polymerase chain reaction (PCR), Western blotting, hematoxylin-eosin (HE) staining, and electron microscopic assessment. Western blotting and RT-qPCR were conducted to identify the mRNA expression levels of PARKIN and PINK-1. Renal tissue morphological changes were observed through HE staining and electron microscopy. The expression of PARKIN, PINK-1, LC3, and NRF-2 was detected using immunohistochemical analysis.

In this investigation, the subsequent substances were employed: Protein Extraction Kit (KGI lot 20220110, China), Protein BCA Quantification Kit (KGI lot 20211020, China), Protein Simple Kit (WES 652020), PARKIN (NBP-29838, Novus Biologicals, LLC, Centennial, CO, USA), and PINK-1 (ER1706-27, HuaBio, Woburn, MA, USA). LC3 (AG5257, Beyotime, CHINA) and NRF-2 (NBP-29838, Novus Biologicals, LLC, Centennial, CO, USA). The RT-PCR primers were utilized according to the information provided in Table 1. Data analysis was conducted using Image J software to confirm the precision of network pharmacology findings.

Preparation of TSF

The composition of TSF consisted of "Huangqi (Radix Astragali seu Hedysari)", "Danggui (Radix Angelicae Sinensis)", "Jixuecao (Centella asiatica (L.) Urb.)", "Fangji (Radix Stephaniae Tetrandrae)", "Taoren (Semen Persicae)", and "Da Huang (Radix et Rhizoma Rhei)" in a proportion of 3:3:3:1:2:1. The ingredients were included in purified water, immersed for half an hour, boiled for half an hour using hydrothermal heat on two occasions, and subsequently strained. The filtered liquid was mixed to acquire a complex water-based extract of TSF with a concentration of 1 gram per milliliter and placed in the refrigerator at a temperature of 20 degrees Celsius.

Statistical Analyses

The information is presented as the average plus the standard error of measurement and was analyzed using IBM Corp.'s SPSS version 25.0 in Armonk, NY, USA. Graphs were generated using GraphPad Prism 9 (GraphPad Software, San Diego, CA, USA) and R software (version 4.0.1). A multiple-group comparison was conducted using an analysis of variance test, assuming that the parameters followed a normal distribution. The level of statistical significance was determined to be less than 0.05, denoted as $P < 0.05$.

Table 1 Primer Sequence

Primer	Sequence (5' to 3')
m PINK1F	TTCTTCCGCCAGTCGGTAG
m PINK1R	CTGCTTCTCCTCGATCAGCC
m PARKINF	GAGGTCGATTCTGACACCAGC
m PARKINR	CCGGCAAAAATCACACGCAG
m GAPDHF	TGTGTCCGTCGTGGATCTGA
m GAPDHR	TTGCTGTTGAAGTCGCAGGAG

Results

TSF Active Compound and Target Gene Screening and Identifying DN Targets

After eliminating duplicates, 44 active constituents of TSF were identified from the TCMSP database (Supplementary Table 1). These include "Huangqi (Radix Astragali seu Hedysari)", "Danggui (Radix Angelicae Sinensis)", "Jixuecao (Centella asiatica (L.) Urb.)", "Fangji (Radix Stephaniae Tetrandrae)", "Taoren (Semen Persicae)", and "Da Huang (Radix et Rhizoma Rhei)". Fifteen components of Huangqi, two components of Danggui, two components of Jixuecao, two components of Fangji, nigh components of Dahuang, eighteen components of Taoren. The prediction of target TSF was conducted using the TCMSP and Swiss Target Prediction databases. The UniProt database was utilized to standardize the names and eliminate duplicates, resulting in 226 marks (Supplementary Table 2). We used OMIM, DisGeNET, DrugBank, and TTD databases to explore the genes associated with "Diabetes kidney disease or Diabetic nephropathy" and the phenotypes related to "Mitophagy" in Homo sapiens (Supplementary Table 3). The cystoscope constructed the drug (TSF)- targets-network, as shown in Figure 2. To create the Venn diagram for the target "TSF-DN-Mitophagy", we utilized the TSF target intersection. We obtained a total of 24 intersection targets. (Figure 3A).

Construction of PPI Network and Network for Component-Target-Disease Interactions Using TSF

The String database imported 24 commonly known TSF and DN targets and mitophagy targets, with a restriction to humans as the species. A high confidence threshold (>0.9) was established to eliminate the irrelevant nodes in the network, resulting in the acquisition of the PPI network graphs for DN and mitophagy in TSF. The PPI network graphs contained 24 nodes and 348 edges, exhibiting an average node degree of 29 and an average local clustering coefficient of 0.806. The top 10 targets were TP53, PTEN, AKT1, BCL2, BCL2L1, HIF1A, MAPK1, TGFB1, MAPK14, PARP1 (Figure 3B and Supplementary Table 4). Cytoscape software was used to construct the "drug (TSF)-components-target-disease (DN and mitophagy)" network and to screen the active components of TSF for DN treatment, as shown in

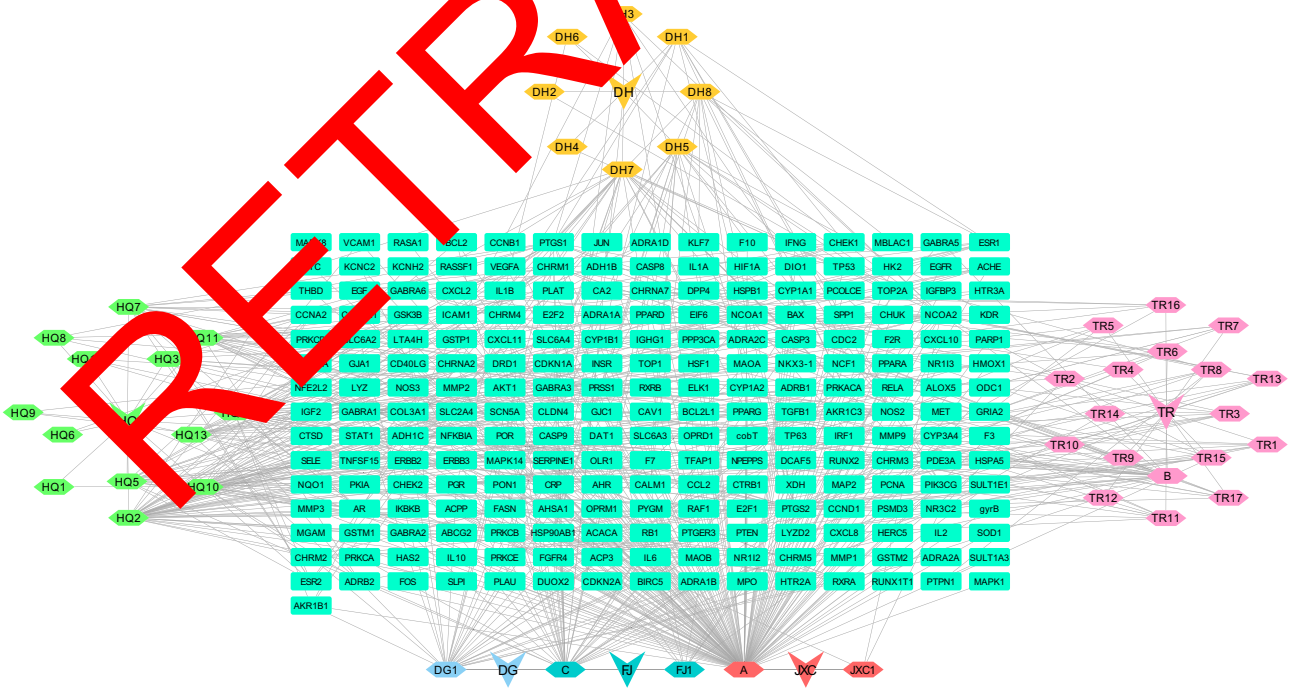

Figure 2 The network of the relationship between the active ingredients and the targets of TSF. A represents the common ingredient that HQ and JXC share. B represents the common ingredient that HQ and TR share. C represents the common ingredient that DG, DH, FJ, and TR share. The rectangle inside each traditional Chinese medicine represents all the gene targets of TSF.

Abbreviations: HQ, huangqi; DH, dahuang; TR, taoren; JXC, jixuecao; FJ, fangji; DG, dangui.

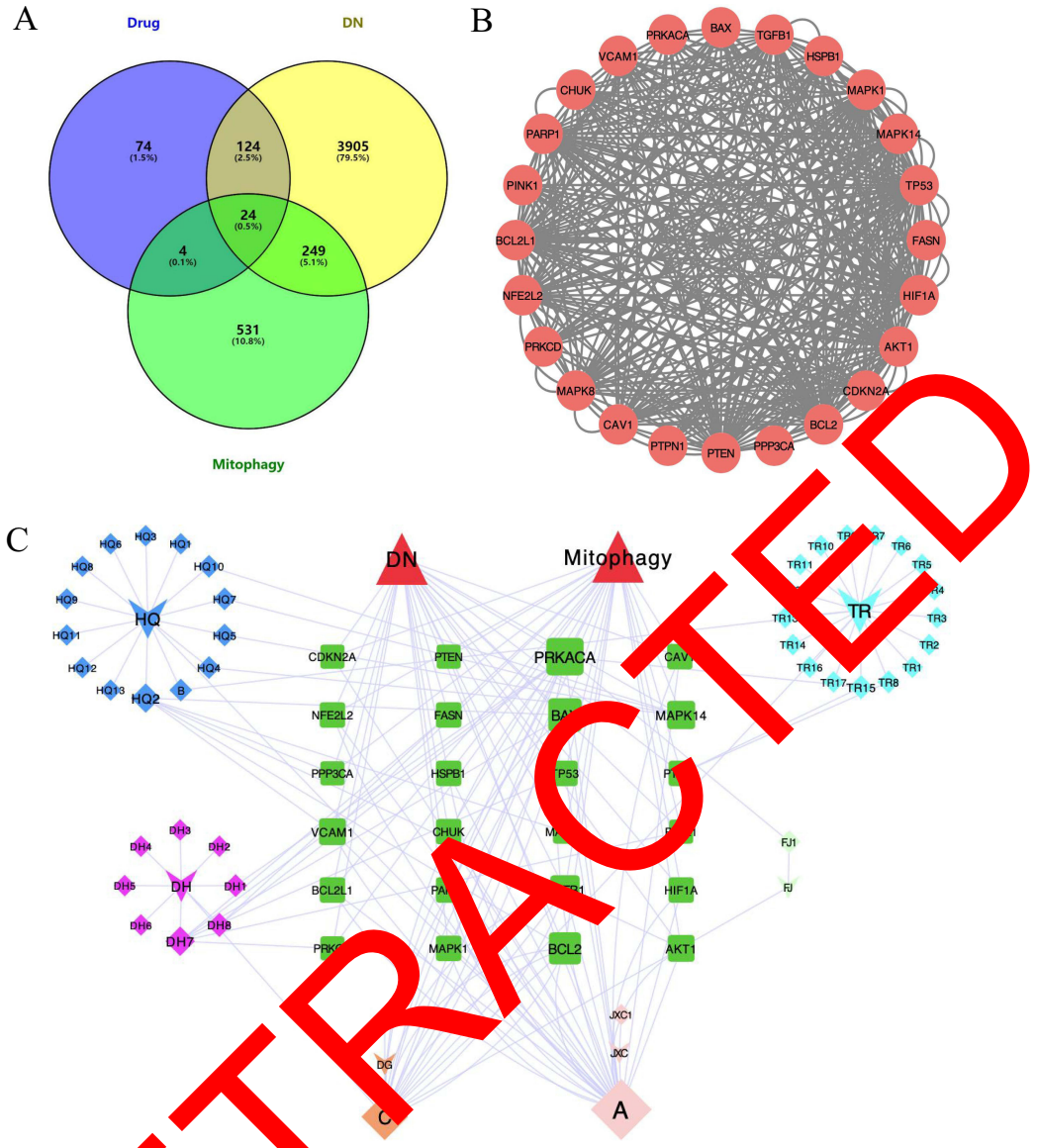

Figure 3 Screening of critical targets in TSF for DN and Mitophagy. (**A**) Venn diagram of targets among DN, TSF and Mitophagy. (**B**) Results of PPI network analysis of TSF interfering with the intersection targets from Venn diagram. (**C**) Through PPI network mapping, results of drug (TSF)-components-target-disease (DN and mitophagy) network. A represents the common ingredient that HQ and JXC share. C represents the common ingredient that DG, DH, FJ, and TR share. The green nodes represent the common targets shared with DN and Mitophagy.
Abbreviations: HQ, huangqi; DH, danhong; TR, taoren; JXC, jixuecao; FJ, fangji; DG, dangui.

Figure 3C. The PPI network had 76 nodes and 166 edges. Quercetin, beta-sitosterol, kaempferol, aloe-emodin, and 3-O-p-coumaroylquinic acid emerged as the leading five compounds, as shown in Table 2.

Enrichment Analysis

The GO enrichment analysis identified a total of 1824 biological processes (BPs), 76 cellular components (CCs), and 94 molecular functions (MFs). The main focus of this work was on the enrichment of BPs in the regulation of pathways that lead to cell death, modification of peptidyl serine, regulation of internal pathways that lead to cell death, response of cells to chemical stress, and internal pathways that lead to cell death; CCs were mainly found at the cytoplasmic side of the membrane, in cell projections bound to the plasma membrane, in cytoplasmic projections of neurons, in the nuclear shell, and in cytoplasmic compartments; MFs primarily included binding to DNA-binding transcription factors, binding to transcription factors specific to RNA polymerase II and DNA, binding to protein phosphatase 2A, activity of forming

Table 2 The 5 Core Ingredients of TSF

Mol ID	Molecule	Struture	OB	DL	Degree	Source
MOL000098	Quercetin	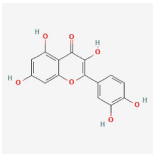	46.43	0.28	31	HQ JXC
MOL000358	Beta-sitosterol	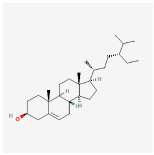	36.91	0.75	20	TR, FJ DH, DG
MOL000422	Kaempferol	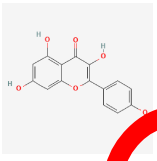	41.88	0.24	7	HQ
MOL000471	Aloe-emodin	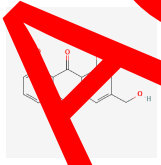	83.38	0.24	7	DH
MOL001368	3-O-[illegible]umaroylquinic [illegible]id	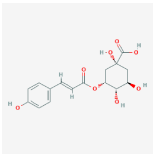	37.86	0.38	3	TR

heterodimer with proteins, and binding to phosphatases (Figure 4A). The analysis of KEGG pathways resulted in 149 pathways that were found to be significant. The five most significant KEGG pathways included the AGE−RAGE signaling pathway in diabetic complications, Apoptosis, Autophagy–animal, Chronic myeloid leukemia, Endocrine resistance, Fluid shear stress, and atherosclerosis Hepatitis B. The target-pathway network was built with the DN-mitophagy-related pathways (Figure 4B, Table 3). Each pathway interacted with the common targets, indicating that TSF could treat DN-mitophagy through multiple pathways.

Molecular Docking

The DN study revealed the involvement of mitochondria and autophagy in multiple biological processes and signal pathways. Molecular docking was performed with the top 5 compounds and the top 5 core targets (TP53, PTEN,

AKT1, BCL2, and BCL2L1), as well as targets associated with mitophagy (PINK-1, PARKIN, LC3B, NFE2L2 [NRF2]). NFE2L2 and NRF2 are two names for a protein. (https://www.genecards.org/). The selection process identified these compounds for the analysis. Typically, a binding energy below −7 signifies a strong attachment of the compound to the target. Molecular docking ability score was shown in Figure 5. The findings indicated that Kaempferol strongly binds to the LC3B target, with a binding energy of −8.9 kcal/mol. It also displayed a similar strong binding affinity to the PARKIN target, with a binding energy of −8.9 kcal/mol. Furthermore, Aloe-emodin demonstrated favorable binding to the PINK1 target. LC3B, PARKIN, and PINK1 exhibited strong affinity for each component from the target's perspective, with a binding energy below −7 kcal/mol. Aloe-emodin and Kaempferol showed a robust binding relationship to all targets except NRF2, a signaling factor, with a binding energy below −7 kcal/mol, as observed from a compound standpoint. The visual analysis findings showed that the compounds were attached to the amino acid pockets of each protein and established hydrogen bonds, van der Waals forces, and Pi-π forces with amino acid residues. (Figure 6) (Supplementary Table 5).

Effect of TSF on Physical and Chemical Tests in DN Mice

The study found that the db/db+vehicle group had significantly higher body weights, blood glucose (Glu), Creatinine (Cr), Total cholesterol (Tch), Urine albumin-creatinine ratio (ACR), Low-Density Lipoprotein (LDL), Triglyceride (TG), and Blood Urea Nitrogen (BUN) levels compared to the normal group (db/m) (P< 0.05). The level of albumin (Alb) was significantly elevated in the db/db+vehicle group compared to the db/m group (normal group) (P< 0.05). Following the administration of TSF medication, both the low dose and high-dose groups

Figure 4 Continued.

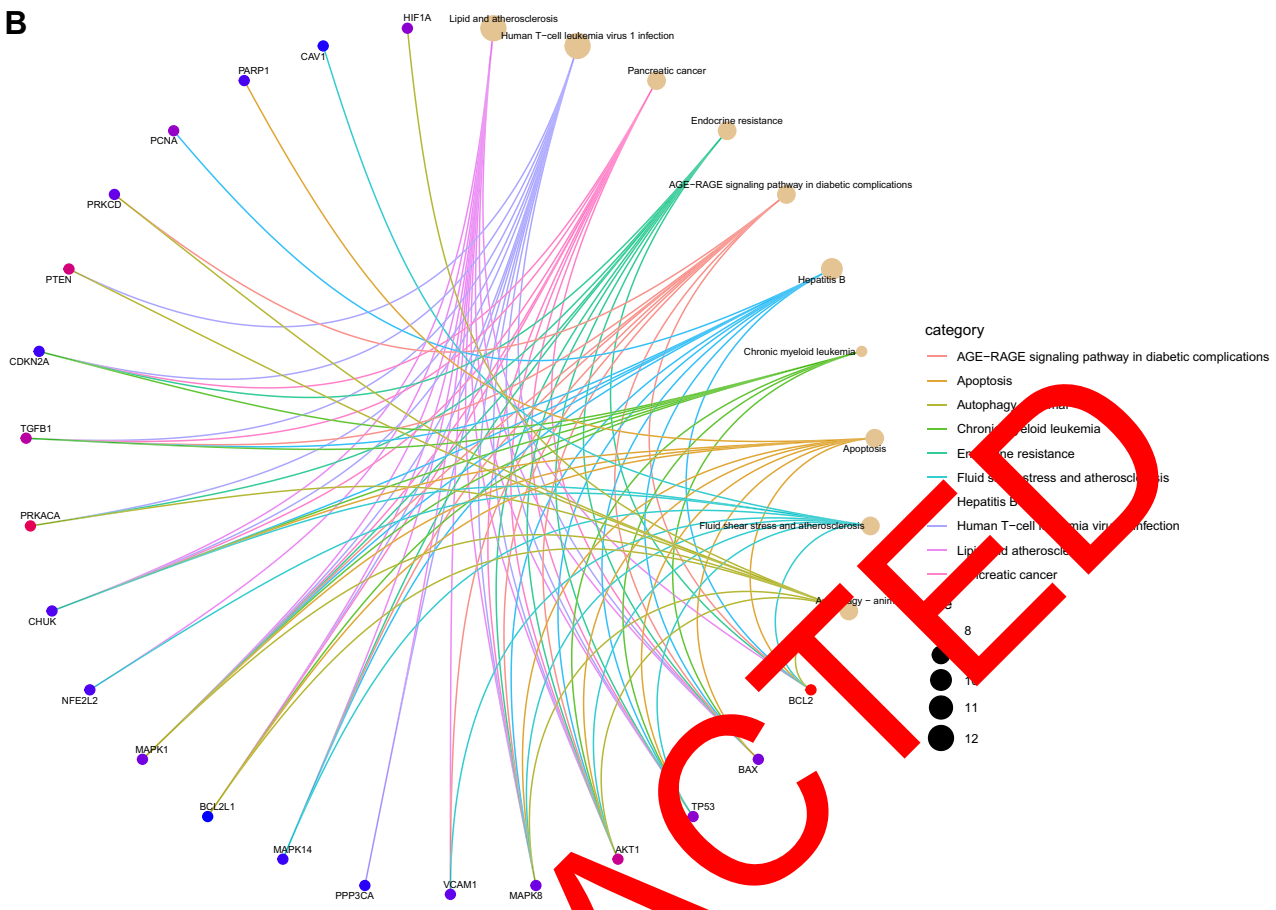

Figure 4 The GO and KEGG enrichment analysis of critical targets. (**A**) The GO enrichment analysis includes Cell assembly [CC], Molecular function [MF] and Biological process [BP]. (**B**) The top 30 KEGG signaling pathways.

exhibited a decrease in Cr, Tch and TG levels compared to the vehicle group (P< 0.05). The levels of Alb were elevated in the db/db+high dose group compared to the db/db+vehicle group (P< 0.05). LDL and BUN levels were reduced in the high-dosage group. The ACR in the dose of TSF remained unchanged when compared to the db/db +vehicle group (Figure 7).

Table 3 The Top 20 Pathways Associated with DN and Mitophagy

ID	Description	Count	pvalue	GeneID
hsa05417	Lipid and atherosclerosis	12	1.54299E-13	BCL2/BAX/TP53/AKT1/MAPK8/VCAM1/PPP3CA/MAPK14/BCL2L1/MAPK1/NFE2L2/CHUK
hsa05166	Human T-cell leukemia virus 1 infection	12	2.26726E-13	PRKACA/BAX/TGFB1/TP53/AKT1/MAPK8/PPP3CA/BCL2L1/MAPK1/CHUK/CDKN2A/PTEN
hsa05212	Pancreatic cancer	9	3.5362E-13	BAX/TGFB1/TP53/AKT1/MAPK8/BCL2L1/MAPK1/CHUK/CDKN2A
hsa01522	Endocrine resistance	9	3.76621E-12	PRKACA/BCL2/BAX/TP53/AKT1/MAPK8/MAPK14/MAPK1/CDKN2A
hsa04933	AGE-RAGE signaling pathway in diabetic complications	9	4.53749E-12	BCL2/BAX/TGFB1/PRKCD/AKT1/MAPK8/VCAM1/MAPK14/MAPK1
hsa05161	Hepatitis B	10	1.03169E-11	BCL2/BAX/TGFB1/TP53/PCNA/AKT1/MAPK8/MAPK14/MAPK1/CHUK
hsa05220	Chronic myeloid leukemia	8	2.38477E-11	BAX/TGFB1/TP53/AKT1/BCL2L1/MAPK1/CHUK/CDKN2A

(*Continued*)

Table 3 (Continued).

ID	Description	Count	pvalue	GeneID
hsa04210	Apoptosis	9	7.52012E-11	BCL2/BAX/TP53/AKT1/MAPK8/BCL2L1/MAPK1/PARP1/CHUK
hsa05418	Fluid shear stress and atherosclerosis	9	9.16067E-11	BCL2/TP53/AKT1/MAPK8/VCAM1/MAPK14/CAV1/NFE2L2/CHUK
hsa04140	Autophagy - animal	9	1.04228E-10	PRKACA/BCL2/PRKCD/AKT1/MAPK8/BCL2L1/MAPK1/HIF1A/PTEN
hsa05208	Chemical carcinogenesis - reactive oxygen species	10	2.47611E-10	PRKCD/AKT1/MAPK8/MAPK14/MAPK1/HIF1A/NFE2L2/CHUK/PTEN/PTPN1
hsa05225	Hepatocellular carcinoma	9	5.0321E-10	BAX/TGFB1/TP53/AKT1/BCL2L1/MAPK1/NFE2L2/CDKN2A/PTEN
hsa05145	Toxoplasmosis	8	5.64739E-10	BCL2/TGFB1/AKT1/MAPK8/MAPK14/[illegible]/CHUK
hsa05131	Shigellosis	10	6.7595E-10	BCL2/BAX/TP53/PRKCD/AKT1/[illegible]/MAPK14/[illegible]/MAPK1/CHUK
hsa04071	Sphingolipid signaling pathway	8	9.20109E-10	BCL2/BAX/TP53/AKT1/[illegible]/MAPK1/[illegible]
hsa04722	Neurotrophin signaling pathway	8	9.20109E-10	BCL2/BAX/TP53/PRKC[illegible]/AKT1/[illegible]/MAPK1
hsa01524	Platinum drug resistance	7	9.94197E-10	BCL2/BAX/TP53/AK[illegible]/BCL2L[illegible]/MAPK1/CDKN2A
hsa05167	Kaposi sarcoma-associated herpesvirus infection	9	1.81211E-09	BAX/TP53/AKT[illegible]/MAPK[illegible]/PPP3CA/MAPK[illegible]/MAPK1/HIF1A/CHUK
hsa05210	Colorectal cancer	7	3.20186E-09	BCL2/BA[illegible]/TGF[illegible]/TP53/AKT1/[illegible]/MAPK8/MAPK1
hsa04010	MAPK signaling pathway	10	3.68884E-09	PRKACA/TGFB1/T[illegible]/AKT1/MAPK8/PPP3CA/MAPK14/[illegible]/HSPB1/CHUK
hsa05235	PD-L1 expression and PD-1 checkpoint pathway in cancer	7	4.08347E-09	[illegible]AKT1/PPP3CA/MAPK14/MAPK1/HIF1A/CHUK/PTEN
hsa05170	Human immunodeficiency virus 1 infection	9	3.97133E-09	[illegible]CL2/BAX/A[illegible]1/MAPK8/PPP3CA/MAPK14/BCL2L1/MAPK1/[illegible]
hsa05222	Small cell lung cancer	7	5.1[illegible]55E-[illegible]	BCL2/BAX/TP53/AKT1/BCL2L1/CHUK/PTEN
hsa05163	Human cytomegalovirus infection	9	6.70[illegible]4E-09	[illegible]CA/BAX/TP53/AKT1/PPP3CA/MAPK14/MAPK1/CHUK/CDKN2A
hsa04218	Cellular senescence	[illegible]	7.97028[illegible]09	TGFB1/TP53/AKT1/PPP3CA/MAPK14/MAPK1/CDKN2A/PTEN
hsa04625	C-type lectin receptor signaling pathway	7	1.22498E-[illegible]8	PRKCD/AKT1/MAPK8/PPP3CA/MAPK14/MAPK1/CHUK
hsa04659	Th17 cell differentiation	7	1.59615E-08	TGFB1/MAPK8/PPP3CA/MAPK14/MAPK1/HIF1A/CHUK
hsa05152	Tuberculosis	8	2.46069E-08	BCL2/BAX/TGFB1/AKT1/MAPK8/PPP3CA/MAPK14/MAPK1
hsa05218	Melanoma	6	4.33288E-08	BAX/TP53/AKT1/MAPK1/CDKN2A/PTEN
hsa04115	p53 signaling pathway	6	4.712E-08	BCL2/BAX/TP53/BCL2L1/CDKN2A/PTEN

Effect of TSF on Morphological Changes in DN

The db/db mice exhibited notable characteristics of DN in HE staining, such as glomerular enlargement and alterations in the thylakoid matrix. The capillary loops revealed inadequate opening, while the tubular epithelial cells appeared swollen and filled with vacuoles. The histological lesions in the db/db+TSF-L (low dose) and db/db+TSF-H groups (high dose) were considerably reduced compared to the vehicle group. Following the implementation of TSF, there was an enhancement in glomerular hypertrophy and an amelioration in the augmented thylakoid matrix compared to the db/db group.

Using an electron microscope, the glomerular podocyte structure and renal tubular mitochondrial ultrastructure were examined in all the mice. Compared to the control group, the group of vehicles exhibited localized thickening of the glomerular basement membrane, disarrayed podocyte formations, and significant swelling along with extensive fusion of podocytes. Following the administration of the medication, there was a notable enhancement in peduncle fusion in both the TSF-L (low dosage) and TSF-H (high dosage) groups compared to the control group. In addition, the group of vehicles exhibited evident damage to the cellular structure, a reduced number of autophagic vesicles, and a disrupted

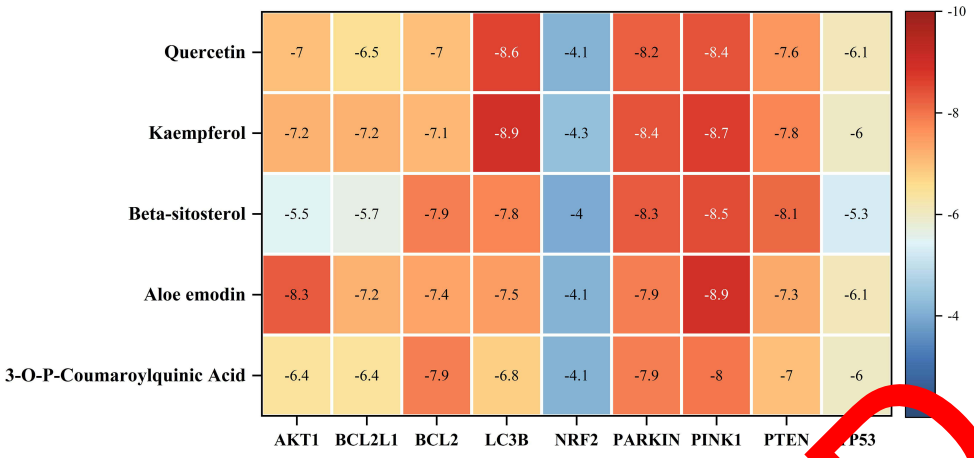

Figure 5 Binding energy heatmap of molecular docking between core ingredients and key targets. Each row represents key targets and columns represent five core ingredients.

organization of mitochondria compared to the normal group. Significantly, there was a varying increase in autophagic vesicles observed in both the low dose and high-dose groups, suggesting a boost in autophagy.

Furthermore, the utilization of transmission electron microscopy revealed distinct autophagic vacuoles surrounding mitochondria in both the low dose and high-dose cohorts, in contrast to the control group. The data suggested that TSF stimulated mitophagy in the DN mice (Figure 8).

The Impact of TSF on the Concentrations of PARKIN/PINK-1, LC3, and NRF-1 in Mice with DN

As shown in Figure 9A and B, the expression levels of PARKIN/PINK-1 in the kidney tissue samples were markedly decreased in the vehicle group compared to the normal group ($P< 0.001$). Following the administration of the medication, there was a notable increase in the expression levels of PINK-1 mRNA in kidney tissue samples from both the low and high dose groups compared to the vehicle group ($P< 0.05$). Furthermore, the mRNA levels of PARKIN exhibited a significant increase in the high-dosage group compared to the vehicle group ($P< 0.05$). As shown in Figure 9C and D, the expression of the PINK-1 protein was higher in the high dose group when compared to the vehicle group. Despite an upward trend in renal PARKIN protein expression in both the low dose and high dose groups compared to the vehicle group, no statistically significant difference was observed. Significantly, the expression of PINK-1 protein in the high dosage group showed a notable increase following treatment compared to the model group ($P< 0.05$). This suggests that TSF triggers mitophagy mediated by PINK-1/PARKIN in db/db mice. Immunohistochemical analysis additionally validated that the TSF treatment notably enhanced the levels of PINK1 and Parkin in the kidney of db/db mice, compared to the control group (Figures 10A, 11A and Figures 10B, 11B). In the kidneys of the normal group, LC3 and NRF-2, commonly used as indicators of mitophagy, were higher than in the vehicle group. Following administration of the medication, LC3 and NRF-2 exhibited an increase in both the low and high-dosage groups, compared to the vehicle group (Figures 10C, 11C and Figures 10D, 11D).

Discussion

This study investigates the mechanism of TSF in treating DN using network pharmacology. TSF has been a commonly prescribed treatment for DN for decades. Nevertheless, further investigation is required to understand the appropriate mechanism. Through screening the TCMSP database and supplementing with literature, 44 potential active components of TSF for treating DN were identified. These components consist of quercetin, beta-sitosterol, kaempferol, aloe-emodin, and 3-O-p-coumaroylquinic acid. Many of the ingredients have been demonstrated to have renoprotective activities. Quercetin is recognized for its significant antioxidant, antiviral, antifibrotic, anti-inflammatory, and anticancer properties.[17–19] Quercetin significantly decreased the renal index, serum/plasma creatinine (SCr), blood urea nitrogen

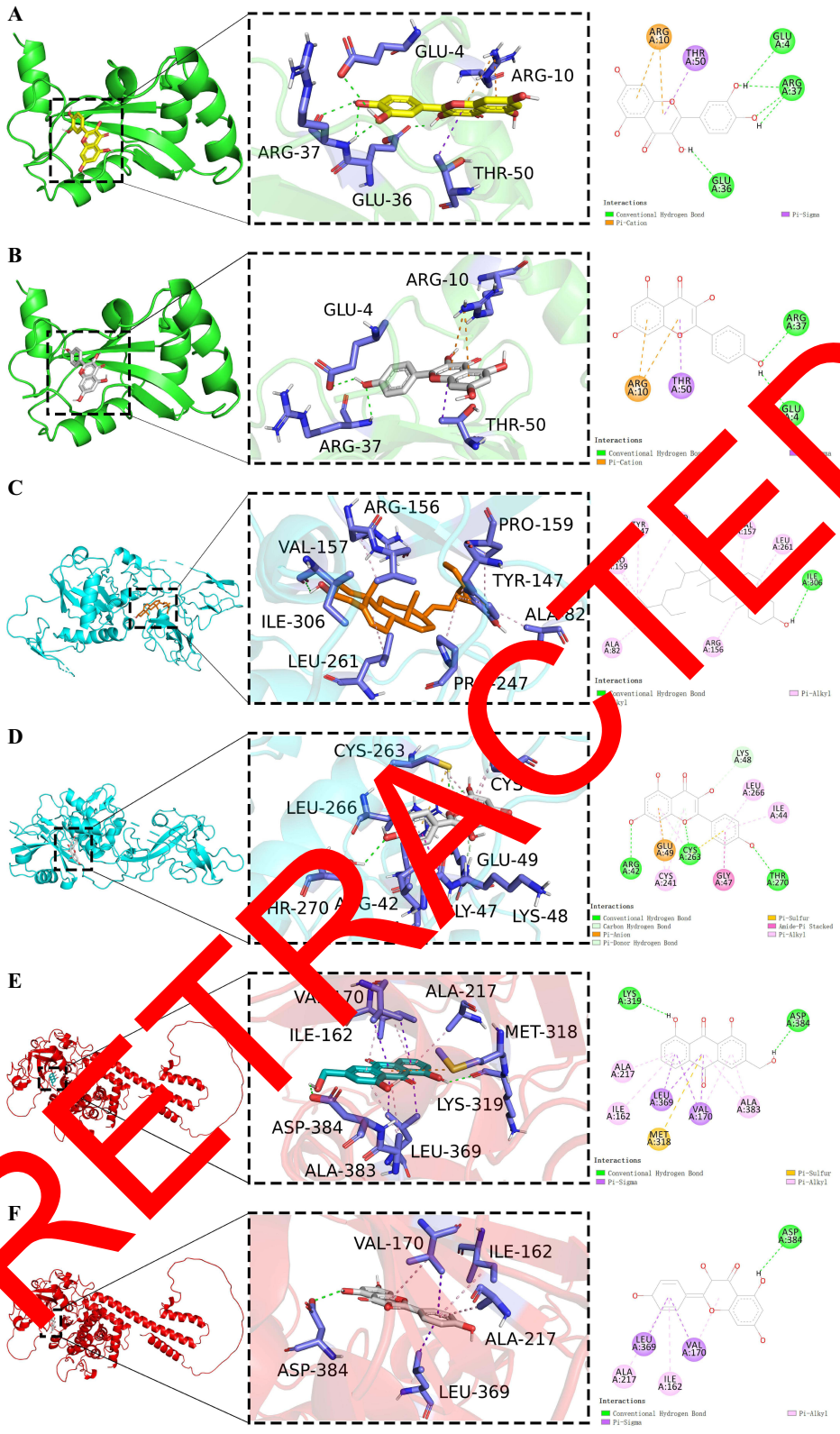

Figure 6 The results of molecular docking between the key ingredients (ligands) and core targets (receptors). (**A**) The binding effect of kaempferol and LC3B (affinity: −8.9). (**B**) The binding effect of quercetin and LC3B (affinity: −8.6). (**C**) The binding effect of PARKIN and beta-sitosterol (affinity: −8.3). (**D**) The binding effect of PARKIN and kaempferol (affinity: −8.7). (**E**) The binding effect of PINK1 and Aloe_emodin (affinity: −8.9). (**F**) The binding effect of PINK1 and kaempferol (affinity: −8.7).

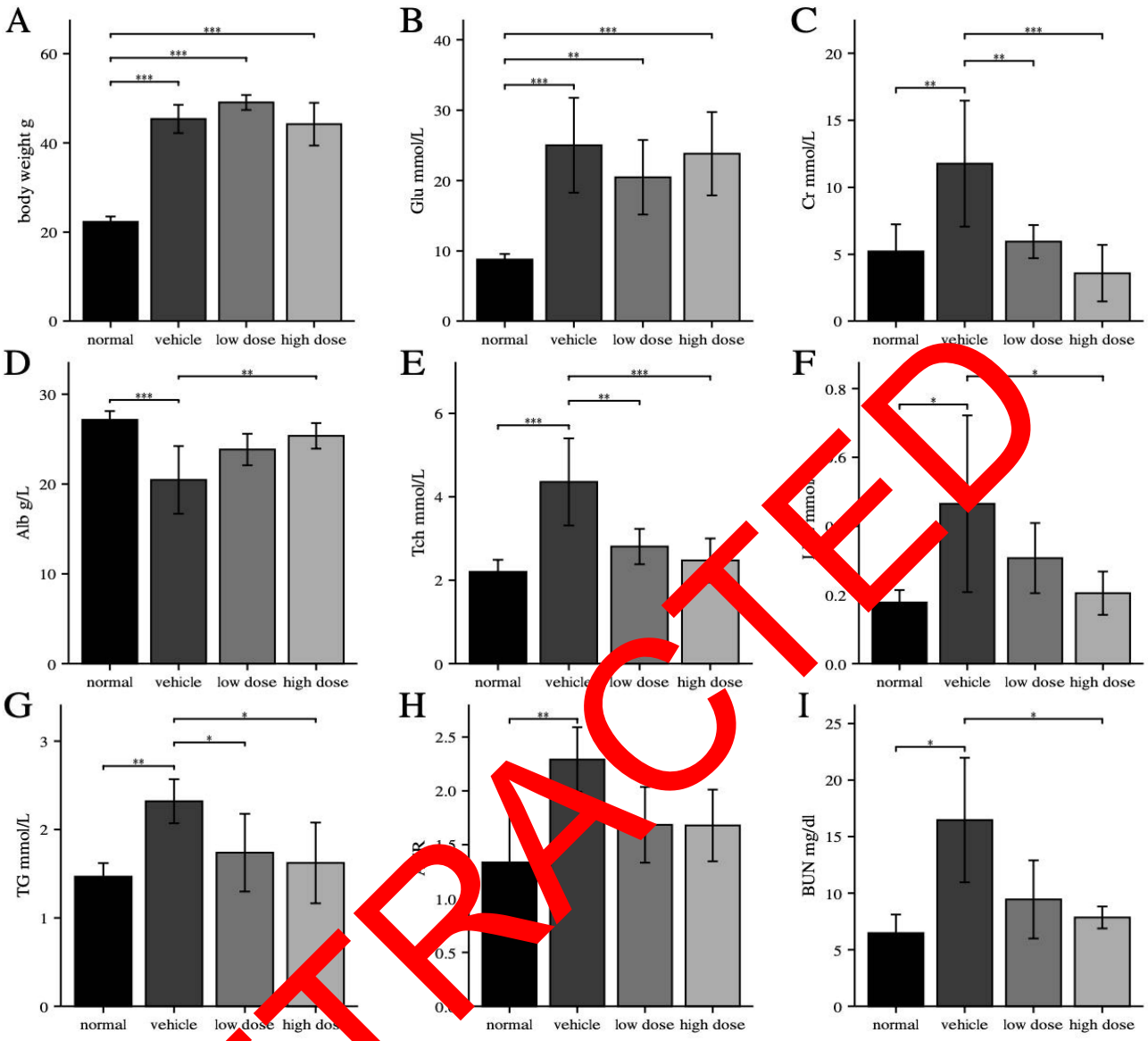

Figure 7 In vivo experiment study of TSF intervention in db/db mice. (**A**) Body weight. (**B**) Blood glucose. (**C**) Serum creatinine. (**D**) Serum albumin. (**E**) Cholesterol. (**F**). LDL. (**G**) Triglycerides. (**H**) ACR (urine protein/urinary creatinine). (**I**) BUN. *** P < 0.001; **P < 0.01; *P<0.05.

(BUN), urinary protein, urinary albumin, malondialdehyde (MDA), tumor necrosis factor (TNF)-α and interleukin (IL)-1β level and increased the activities of superoxide dismutase (SOD) and catalase (CAT) in DN animal models.[20,21] The effects of high glucose in human mesangial cell cultures are partially suppressed by Quercetin, which involves the suppression of NF-κB to some extent.[22] Kaempferol is a natural polyflavonol that has antidiabetic therapeutics. Earlier studies demonstrated that Kaempferol protects the kidneys and reduces fibrotic effects in DN. It achieves this by regulating TRAF6, thereby alleviating inflammatory responses in DN.[23] Aloe-emodin, an anthraquinone type, can be discovered in aloe, rhubarb, cassia seed, and other Chinese herbal plants.[24] Aloe-emodin significantly inhibited the production of NO, IL-6 and IL-6 1β in LPS-stimulated RAW 264.7 cells.[25] It also inhibited the protein expression of inducible nitric oxide synthase, the degradation of IκBα, and the phosphorylation of ERK, p38, JNK and Akt.[25] The pharmacological effect is strongly linked to eliminating oxygen free radicals and the biological activities against tumors.[26] Aloe-emodin can bind with mTORC2 and inhibit its kinase activity.[27] Aloe-emodin exerts antiproliferation effects and induces cellular apoptosis.[28] A recent experiment conducted in vivo showed that aloe-emodin has the

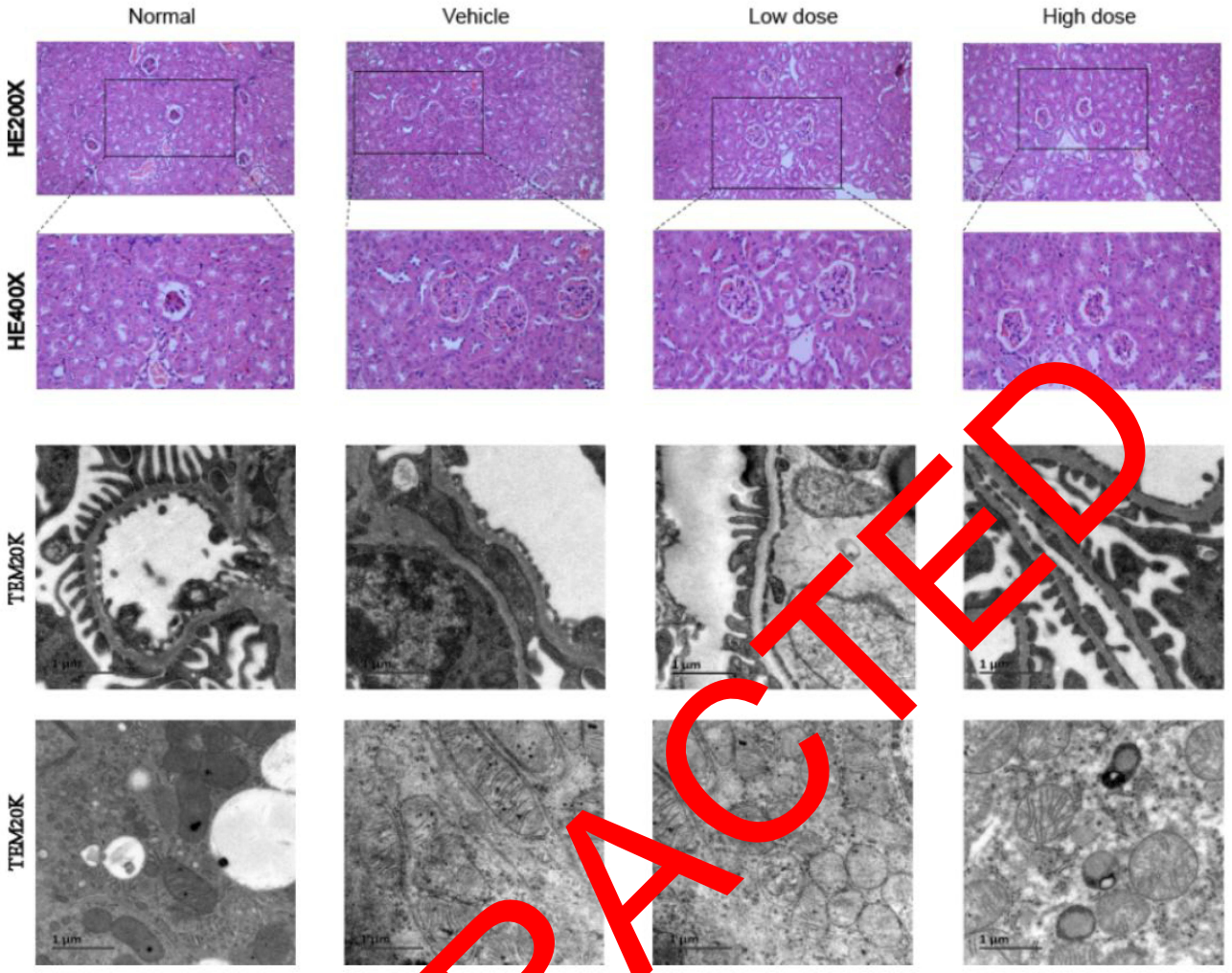

Figure 8 Changes of HE staining and ultrastructural pathology. Histo- pathological changes of the kidney observed by light microscopy under HE staining in the normal, model, low-dose YHQD and high-dose YHQD groups and ultrastructure of glomerular pedicle cells and renal tubular mitochondria under electron microscopy.

potential to improve DN by specifically targeting IRF4, as indicated by a recent study.[29] The results provide evidence for the nephroprotective effects of the potent constituents of TSF.

Analysis of the interaction between the primary components of TSF and the targets of DN and mitophagy indicates that TSF may address DN by targeting crucial factors like PINK-1 and PARKIN. During the enrichment analysis, the main objectives showed significant enrichment in signaling pathways related to Autophagy, such as the pathway involving PINK-1 and PARKIN. Based on the results of network pharmacology, TSF has the potential to inhibit DN through the process of mitochondrial autophagy mediated by PINK-1/PARKIN. The PINK-1/PARKIN signaling pathway is a significant pathway that controls the function of mitochondrial autophagy.[30,31] PINK-1, a mitochondrial protein kinase, initiates mitochondrial autophagy and acts as a sensor for damaged mitochondria, while PINK-1 recruits PARKIN into damaged mitochondria.[32] Molecular docking was conducted to confirm the impact of TSF on mitophagy targets. The top 5 active compounds of TSF and targets of mitophagy were interconnected, respectively. The results indicated that TSF may significantly impact the PINK-1/PARKIN signaling pathway in DN, as the five active compounds exhibited favorable docking activities with autophagy-related targets, particularly PINK1, PAKIN, and LC3B. Hence, additional validation tests are required to uncover the impact and mechanism of TSF.

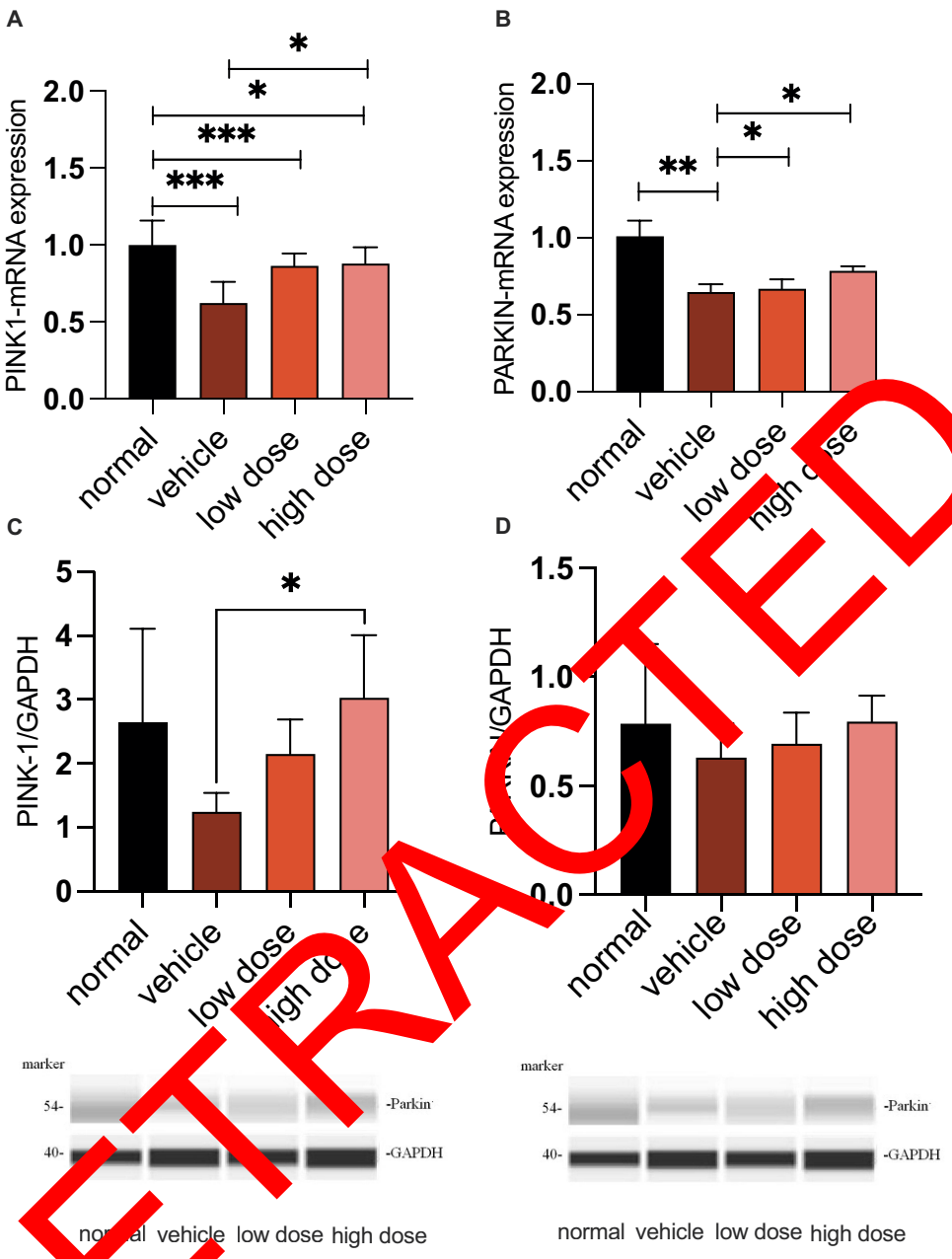

Figure 9 Changes of PINK1 and PARKIN mRNA and protein levels in the kidney tissues in each group. (**A**) mRNA expression of PINK-1. (**B**) mRNA expression of PARKIN. (**C**) protein expression of PINK-1. (**D**) protein expression of PARKIN. *** P < 0.001; **P < 0.01; *P < 0.05.

Consequently, in this study, TSF was administered to db/db mice as a representative animal model of DN. Following the treatment, the levels of Cr, Tch, LDL, TG, BUN, and ACR in db/db mice showed a noticeable decrease, while the levels of Alb exhibited a significant increase compared to the model group. Significantly, in the kidney pathology, we observed a reduction in glomerular hypertrophy and thylakoid matrix in db/db mice following TSF treatment, compared to the model group. Compared to the model group, the electron microscope revealed notable enhancements in peduncle fusion and a higher abundance of autophagic vesicles in db/db mice.

Furthermore, this investigation demonstrated that TSF enhanced the expression of PINK1, Parkin, LC3, and NRF-2, which are proteins associated with mitophagy and promoted mitophagy itself. The involvement of PINK1/Parkin signaling pathways in mitochondrial damage and autophagic clearance is now supported by compelling evidence.[33] PINK1 is recognized for its buildup on the external layer of mitochondria and its role in assisting the transfer of Parkin

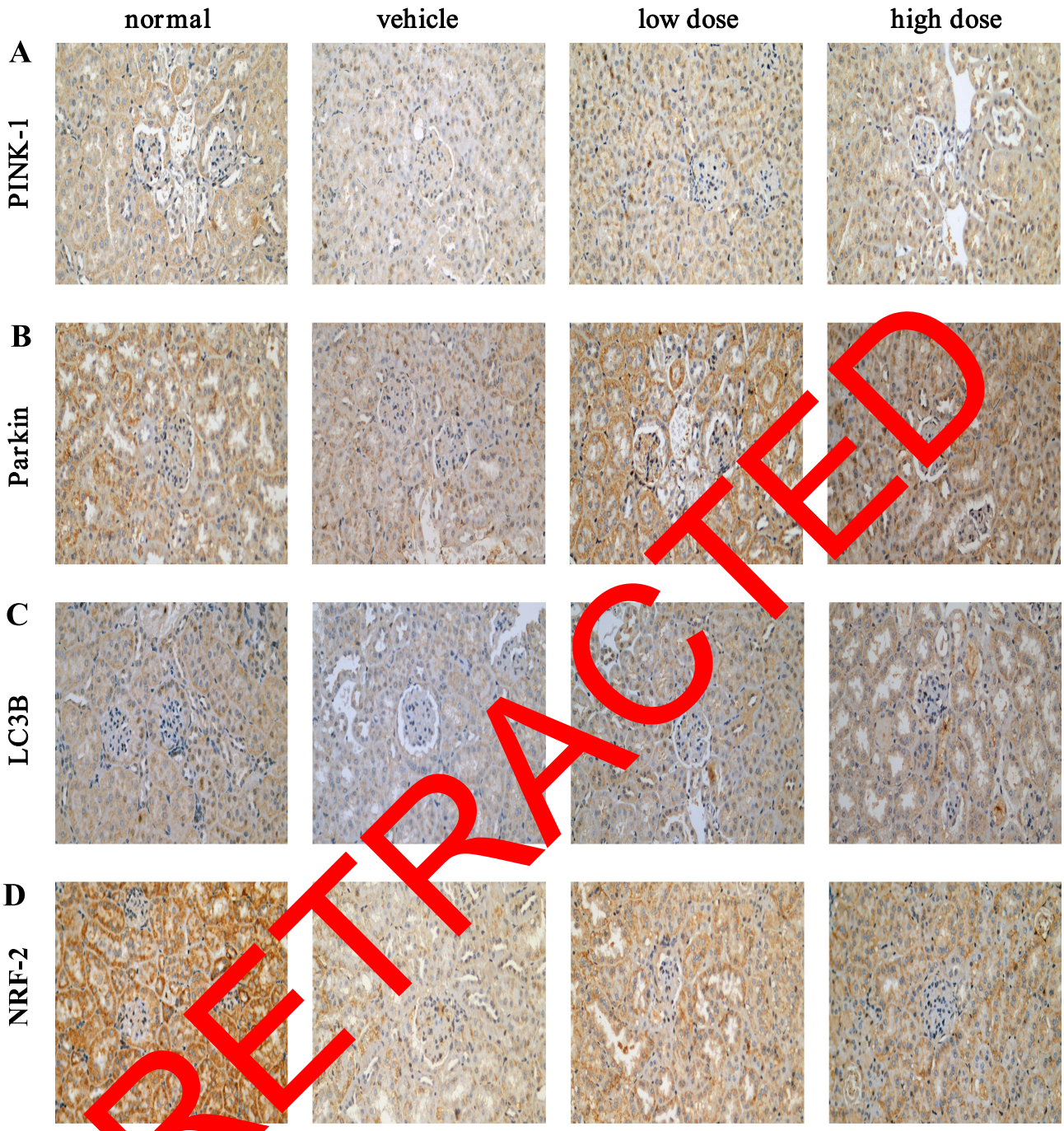

Figure 10 Immunohistochemical staining for each group in kidney tissues. (**A**) PINK1. (**B**) Parkin. (**C**) LC3B. (**D**) NRF2.

from the cytoplasm to the mitochondria. The recruiting process leads to the ubiquitination of different substances, resulting in the improved removal of damaged mitochondria through autophagy.[34] Under conditions of low oxygen levels, the LC3-binding domain (LBD) of BNIP3 and Nix binds to LC3 on the membrane of the autophagosome, leading to an elevation in the phosphorylation of serine residues adjacent to the LBD region.[32,33] The conversion of LC3-I to LC3-II[34] occurs during this process. The above findings concluded that TSF could potentially hinder autophagy and mitophagy, thereby preventing diabetic kidney injury. In vivo experiments confirmed the validity of the TSF protective effect and its ability to inhibit autophagy and mitophagy in treating diabetic kidney injury.

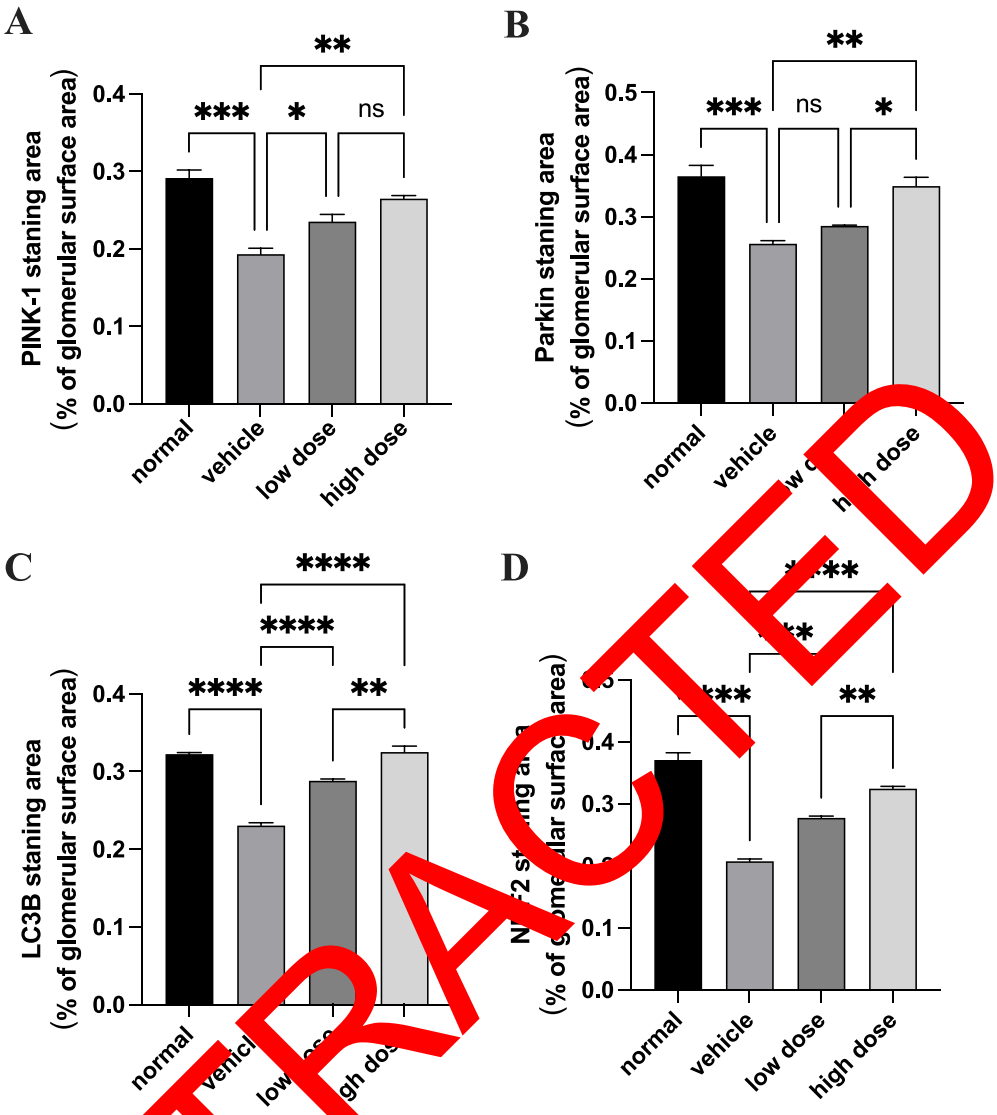

Figure 11 Semi-quantitative results of immunohistochemical analysis for each group in kidney tissues. (**A**) PINK1. (**B**) Parkin. (**C**) LC3B. (**D**) NRF2. *P < 0.05; **P < 0.01; ***P < 0.005; ****Represents a P < 0.001.

Conclusion

In this db/db mice study, the expression of PINK-1/PARKIN in the mitochondrial autophagic pathway was increased by TSF. This discovery suggests that TSF could trigger mitochondrial autophagy, potentially enhancing clinical results. This research proposes that TSF holds promise for therapeutic use in db/db mice by activating PINK-1/PARKIN-mediated mitophagy. TSF reduced urinary protein levels, improved renal function, and inhibited pathological renal damage.

Statement of Authorship Contribution According to CRediT

All authors made a significant contribution to the work reported, whether that is in the conception, study design, execution, acquisition of data, analysis and interpretation, or in all these areas; took part in drafting, revising or critically reviewing the article; gave final approval of the version to be published; have agreed on the journal to which the article has been submitted; and agree to be accountable for all aspects of the work.

Funding

The research was funded by the Zhejiang Traditional Medicine and Technology Program for Young Scholars, China (Grant No.2020ZQ040) and the China Association of Traditional Chinese Medicine for the promotion of the Young Talents project (2022-QNRC2-B21).

Disclosure

The authors report no conflicts of interest in this work.

References

1. Tuttle KR, Bakris GL, Bilous RW, et al. Diabetic kidney disease: a report from an ADA Consensus Conference. *Am J Kidney Dis Care*. 2014;37(10):2864–2883. PMID: 25249672. doi:10.2337/dc14-1296
2. Cho NH, Shaw JE, Karuranga S, et al. IDF Diabetes Atlas: global estimates of diabetes prevalence for 2017 and projections for 2045. *Diabet Res Clin Pract*. 2018;138:271–281. PMID: 29496507. doi:10.1016/j.diabres.2018.02.023
3. Zhang L, Long J, Jiang W, et al. Trends in chronic kidney disease in China. *N Engl J Med*. 2016;375(9):905–906. PMID: 27579659. doi:10.1056/NEJMc1602469
4. Yamazaki T, Mimura I, Tanaka T, Nangaku M. Treatment of diabetic kidney disease: current and future. *Diabetes Metab J*. 2021;45(1):11–26. PMID: 33508907. doi:10.4093/dmj.2020.0217
5. Hu Q, Chen Y, Deng X, et al. Diabetic nephropathy: focusing on pathological signals, clinical treatment, and dietary regulation. *Biomed Pharmacother*. 2023;159:114252. PMID: 36641921. doi:10.1016/j.biopha.2023.114252
6. Singh DK, Winocour P, Farrington K. Oxidative stress in early diabetic nephropathy: fanning the fire. *Nat Rev Endocrinol*. 2011;7(3):176–184. PMID: 21151200. doi:10.1038/nrendo.2010.212
7. Yao L, Liang X, Qiao Y, Chen B, Wang P, Liu Z. Mitochondrial dysfunction in diabetic tubulopathy. *Metabolism*. 2022;131:155195. PMID: 35358497. doi:10.1016/j.metabol.2022.155195IF:13.934Q1
8. Zhang X, Feng J, Li X, et al. Mitophagy in diabetic kidney disease. *Front Cell Dev Biol*. 2021;9:778011. PMID: 34957109. doi:10.3389/fcell.2021.778011
9. Terešak P, Lapao A, Subic N, Boya P, Elazar Z, Simonsen A. Regulation of PINK1-independent mitophagy. *Autophagy*. 2022;18(1):24–39. PMID: 33570005. doi:10.1080/15548627.2021.1888244
10. Tang C, Livingston MJ, Liu Z, Dong Z. Autophagy in kidney homeostasis and disease. *Nat Rev Nephrol*. 2020;16(9):489–508. PMID: 32704047. doi:10.1038/s41581-020-0309-2
11. Chacko BK, Reily C, Srivastava A, et al. Prevention of diabetic nephropathy in Ins2+/−AkitaJ mice by the mitochondria-targeted therapy MitoQ. *Biochem. J*. 2010;432(1):9–19. doi:10.1042/BJ20100396
12. Wen D, Tan RZ, Zhao CY, et al. Astragalus mongholicus Bunge and Panax notoginseng (Burkill) F.H. Chen Formula for renal injury in diabetic nephropathy-in vivo and in vitro evidence for autophagy regulation. *Front Pharmacol*. 2020;11:732. PMID: 32595492; PMCID: PMC7303297. doi:10.3389/fphar.2020.00732
13. Hu S, Wang J, Liu E, et al. Protective effect of berberine in diabetic nephropathy: a systematic review and meta-analysis revealing the mechanism of action. *Pharmacol Res*. 2022;185:106481. PMID: 36307307. doi:10.1016/j.phrs.2022.106481
14. Liu X, Liu L, Chen P, et al. Clinical trials of traditional Chinese medicine in the treatment of diabetic nephropathy—a systematic review based on a subgroup analysis. *J Ethnopharmacol*. 2014;151(2):810–819. PMID: 24296085. doi:10.1016/j.jep.2013.11.028
15. Zhu Q, Chen H, Zeng J. Effect of compound centella asiatica on renal protection and expression of heme oxygenase-1 and NADPH oxidase 4 in rats with diabetic nephropathy. *Chin J Integr Trad Chin Western Med Nephrol*. 2021;22(02):111–115+190.
16. Hopkins AL. Network pharmacology: the next paradigm in drug discovery. *Nat Chem Biol*. 2008;4(11):682–690. PMID: 18936753. doi:10.1038/nchembio.118
17. Li Y, Yao J, Han C, et al. Quercetin, inflammation and immunity. *Nutrients*. 2016;8(3):167. PMID: 2699919. doi:10.3390/nu8030167
18. Marcolin E, San-Miguel B, Vallejo D, et al. Quercetin treatment ameliorates inflammation and fibrosis in mice with nonalcoholic steatohepatitis. *J Nutr*. 2012;142(10):1821–1828. PMID: 22915297. doi:10.3945/jn.112.165274
19. Boots AW, Haenen GR, Bast A. Health effects of quercetin: from antioxidant to nutraceutical. *Eur J Pharmacol*. 2008;585(2–3):325–337. PMID: 18417116. doi:10.1016/j.ejphar.2008.03.008
20. Chen P, Shi Q, Hong X, Wang Y, Chen W, Wang H. Quercetin suppresses NF-κB and MCP-1 expression in a high glucose-induced human mesangial cell proliferation model. *Int J Mol Med*. 2012;30(1):119–125. PMID: 22469745. doi:10.3892/ijmm.2012.955
21. Luo W, Chen X, Ye L, et al. Kaempferol attenuates streptozotocin-induced diabetic nephropathy by downregulating TRAF6 expression: the role of TRAF6 in diabetic nephropathy. *J Ethnopharmacol*. 2021;268:113553. PMID: 33152432. doi:10.1016/j.jep.2020.113553
22. Si TL, Liu Q, Ren YF, et al. Enhanced anti-inflammatory effects of DHA and quercetin in lipopolysaccharide-induced RAW264.7 macrophages by inhibiting NF-κB and MAPK activation. *Mol Med Rep*. 2016;14(1):499–508. PMID: 27176922. doi:10.3892/mmr.2016.5259
23. Sharma D, Kumar Tekade R, Kalia K. Kaempferol in ameliorating diabetes-induced fibrosis and renal damage: an in vitro and in vivo study in diabetic nephropathy mice model. *Phytomedicine*. 2020;76:153235. PMID: 32563017. doi:10.1016/j.phymed.2020.153235
24. Arosio B, Gagliano N, Fusaro LMP, et al. Aloe-emodin quinone pretreatment reduces acute liver injury induced by carbon tetrachloride. *Pharmacol Toxicol*. 2008;87(5):229–233. PMID: 11129503. doi:10.1034/j.1600-0773.2000.pto870507.x
25. Hu B, Zhang H, Meng X, Wang F, Wang P. Aloe-emodin from rhubarb (Rheum rhabarbarum) inhibits lipopolysaccharide-induced inflammatory responses in RAW264.7 macrophages. *J Ethnopharmacol*. 2014;153(3):846–853. PMID: 24685589. doi:10.1016/j.jep.2014.03.059
26. Wamer WG, Vath P, Falvey DE. In vitro studies on the photobiological properties of aloe emodin and aloin A. *Free Radic Biol Med*. 1997;23(6):851–858. PMID: 12521605. doi:10.1016/s0891-5849(97)00068-3

27. Liu K, Park C, Li S, et al. Aloe-emodin suppresses prostate cancer by targeting the mTOR complex 2. *Carcinogenesis*. 2012;33(7):1406–1411. PMID: 22532249. doi:10.1093/carcin/bgs156
28. Wu YY, Zhang JH, Gao JH, Li YS. Aloe-emodin (AE) nanoparticles suppresses proliferation and induces apoptosis in human lung squamous carcinoma via ROS generation in vitro and in vivo. *Biochem Biophys Res Commun*. 2017;490(3):601–607. PMID: 28629998. doi:10.1016/j.bbrc.2017.06.084
29. Lu L, Li Y, Yuan Y. Aloe-Emodin Ameliorates Diabetic Nephropathy by targeting interferon regulatory factor 4. *Evid Based Complement Alternat Med*. 2022;2022:2421624. PMID: 35518350. doi:10.1155/2022/2421624
30. Cherra SJ 3rd, Dagda RK, Tandon A, Chu CT. Mitochondrial autophagy as a compensatory response to PINK1 deficiency. *Autophagy*. 2009;5(8):1213–1214. PMID: 19786829. doi:10.4161/auto.5.8.10050
31. Vives-Bauza C, Zhou C, Huang Y, et al. PINK1-dependent recruitment of Parkin to mitochondria in mitophagy. *Proc Natl Acad Sci U S A*. 2010;107(1):378–383. PMID: 19966284. doi:10.1073/pnas.0911187107
32. Nguyen TN, Padman BS, Lazarou M. Deciphering the molecular signals of PINK1/Parkin mitophagy. *Trends Cell Biol*. 2016;26(10):733–744. PMID: 27291334. doi:10.1016/j.tcb.2016.05.008
33. González-Rodríguez P, Klionsky DJ, Joseph B. Autophagy regulation by RNA alternative splicing and implications in human diseases. *Nat Commun*. 2022;13(1):2735. PMID: 35585060. doi:10.1038/s41467-022-30433-1
34. Kabeya Y, Mizushima N, Ueno T, et al. LC3, a mammalian homologue of yeast Apg8p, is localized in autophagosome membranes after processing. *EMBO J*. 2000;19(21):5720–5728. PMID: 11060023. doi:10.1093/emboj/19.21.5720